Supplementary Information

The Electron and Spin Distributions and Magnetic Anisotropy in Mixed-Valent Diruthenium(V) Tetracarboxylates from Crystallography and Theory

Sabrina Grenda*,[a], Haruki Yairi[b], Torao Fujimoto[b], Oscar Fabelo,[c] Iurii Kibalin,#[c] Nicolas Claiser,[e] Rémi Maurice,[f] Arsen Gukasov,[d] Laura Canadillas-Delgado,[c] José A. Rodriguez Velamazan,[c] Jean-François Jacquot,[g] Ryoji Mitsuhashi,#[h] Masahiro Mikuriya,[h] Makoto Handa*,[b] and Dominique Luneau*[a]

Table of contents

1. Synthesis

Tetra(*n*-butyl)ammonium salt of dibromotetrakis(μ-*n*-butyrato-*O*,*O'*)diruthenate(II,III), $(NBu_4)[Ru_2^V(O_2CC_3H_7)_4Br_2]$. The starting material, $[Ru_2(O_2CC_3H_7)_4Br]$, was prepared according to a method described in the previous paper.[1] 63.1 mg (0.1 mmol) of $[Ru_2(O_2CC_3H_7)_4Br]$and 32.9 mg (0.1 mmol) of $(n\text{-}C_4H_9)_4NBr$ were dissolved in 20 mL of dichloromethane and the mixed solution was refluxed for 24 h. Then, the reaction solution was concentrated by evaporation to give a reddish-brown precipitate, which was filtered off and dried under vacuum at 353 K for 3 h. The yield was 87.4 mg (91.6% based on $[Ru_2(O_2CC_3H_7)_4Br]$). Anal. Found: C, 40.33; H, 6.30; N, 1.61%. Calculated for $C_{32}H_{64}Br_2NO_8Ru_2$: C, 40.34; H, 6.77; N, 1.47%. IR (KBr, cm^{-1}): ν(CH) 2964, 2934, 2874; ν(COO^-) 1464, 1425, 1415.

2. Crystal growing

Large crystals for neutron diffraction (3.5x2.5x1.5mm) were grown after 2-3 days by slow diffusion of ethylic ether (Et_2O) in a saturated solution of the diruthenium compound in CH_2Cl_2 at ambient temperature (T=25-30°C).

3. High-resolution X-Ray diffraction crystal structure

High-resolution X-ray diffraction data were collected on an Oxford Diffraction SuperNova diffractometer using a single cubic-like crystal (0.10 x 0.09 x 0.11 mm^3). The measurements were performed at 100K using an Oxford Cryosystems N_2 cooling device. The data collection strategy, reflections indexation, intensity integration and absorption correction were carried out using the program CRYSALIS [2]. The merging of the data was carried out with SORTAV [3]. The structures were solved by intrinsic phasing method using the SHELXT program[4] and they were refined using the Independent Atom Model

(IAM) by full matrix least-square methods on F^2 with the 2018 version of SHELXL program[5] incorporated in OLEX2 software.[6] All non-hydrogen atoms were refined with anisotropic displacement parameters. Hydrogen atoms belonging to carbon atoms were placed geometrically in their idealized positions and refined using a riding model. Main crystal data and structure refinement parameters are displayed in Table S1 and selected interatomic distances and angles are listed in Table S2. CCDC deposition number 2516707 contains the supplementary X-ray crystallographic data. These data can be obtained free of charge via www.ccdc.cam.ac.uk/data_request/cif, or by emailing data_request@ccdc.cam.ac.uk, or by contacting The Cambridge Crystallographic Data Centre, 12 Union Road, Cambridge CB2 1EZ, UK; fax: +44 1223 336 033.

Table S1: Crystal data and structure refinement parameters

	High-resolution X-ray diffraction	Neutron diffraction
CCDC number	2516707	2519322
Empirical formula	$C_{16}H_{28}Br_2O_8Ru_2.C_{16}H_{36}N$	$C_{16}H_{28}Br_2O_8Ru_2.C_{16}H_{36}N$
Formula weight/g.mol^{-1}	952.80	952.80
Temperature/K	100(2)	2(2)
Crystal system	triclinic	triclinic
Space group	*P*	*P*
a/Å	12.18040(10)	12.1649(18)
b/Å	12.57170(10)	12.5424(19)
c/Å	14.13050(10)	14.114(2)
α/°	98.2620(10)	98.537(15)
β/°	95.2130(10)	95.070(14)
γ/°	109.9310(10)	109.360(10)
Volume/Å^3	1990.19(3)	1987.2(6)
Z	2	2
ρ_{calc} gcm^{-3}	1.590	1.592
μ/mm^{-1}	2.811	0.251
F(000)	970	114.0
Crystal size/mm^3	0.10× 0.09 × 0.11	3.5 × 2.5 × 1.5
Radiation /Å	MoKα (λ = 0.71073)	Neutron (λ = 0.950)
2Θ range for data collection/°	3.508 to 99.456	9.31 to 122.382
Reflections collected	580963	32546
Independent reflections	40849	15283
Data/restraints/parameters	40849/0/427	15283/0/1048
Goodness-of-fit on F^2	1.058	1.123
Final R indexes [I>=2σ (I)]	R1 = 0.0287, wR2 = 0.0624	R1 = 0.0847, wR2 = 0.1188
Final R indexes [all data]	R1 = 0.0455, wR2 = 0.0665	R1 = 0.1174, wR2 = 0.1245
Largest diff. peak/hole / e.Å^{-3}	1.542/-1.731	1.60/-1.28

Table S2. Selected interatomic distances (Å) and angles (°) at 100K from X-ray diffraction.

Ru1A	Ru1A[1]	2.3108(3)	Ru1B	Ru1B[2]	2.3054(4)
Ru1A	Br1A	2.6555(3)	Ru1B	Br1B	2.6593(4)
Ru1A	O1A	2.0287(7)	Ru1B	O1B	2.0236(6)
Ru1A	O2A[1]	2.0313(6)	Ru1B	O2B[2]	2.0321(6)
Ru1A	O3A	2.0257(6)	Ru1B	O3B	2.0302(6)
Ru1A	O4A[1]	2.0370(6)	Ru1B	O4B[2]	2.0337(6)
O1A	O2A	2.240(1)	O1B	O2B	2.240(1)
O3A	O4A	2.241(1)	O3B	O4B	2.241(1)
O1A	C1A	1.269(1)	O1B	C1B	1.271(1)
O2A	C1A	1.271(1)	O2B	C1B	1.274(1)
O3A	C5A	1.269(1)	O3B	C5B	1.270(1)
O4A	C5A	1.271(1)	O4B	C5B	1.271(1)

O1A	Ru1A	Br1A	92.93(2)	O1B	Ru1B	Br1B	91.53 (2)
O1A	Ru1A	O2A[1]	177.83(2)	O1B	Ru1B	O2B[2]	178.08(2)
O1A	Ru1A	O3A	91.13(3)	O1B	Ru1B	O3B	90.62(3)
O1A	Ru1A	O4A[1]	87.81(3)	O1B	Ru1B	O4B[2]	88.42(3)
O2A[#]	Ru1A	Br1A	89.08 (2)	O2B[#]	Ru1B	Br1B	90.31(2)
O2A[#]	Ru1A	O4A[1]	92.94(3)	O2B[#]	Ru1B	O4B[2]	92.05(3)
O3A	Ru1A	Br1A	91.22(2)	O3B	Ru1B	Br1B	89.34(2)
O3A	Ru1A	O2A[1]	88.03(3)	O3B	Ru1B	O2B[2]	88.85(3)
O3A	Ru1A	O4A[1]	177.77(3)	O3B	Ru1B	O4B[2]	177.94(2)
O4A[#]	Ru1A	Br1A	90.81(2)	O4B[#]	Ru1B	Br1B	92.50(2)

[1]-x,1-y,2-z; [2]1-x,-y,1-z

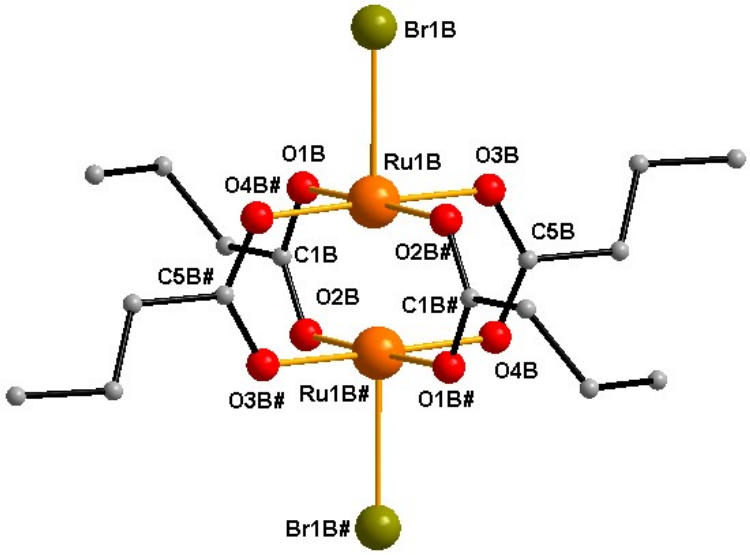

Figure S1: Representation of the $[Ru_2^{V}Br_2(O_2CC_3H_7)_4]^-$ cation complex unit labelled B. Hydrogen atoms have been omitted for clarity, # -x, -y, -z.

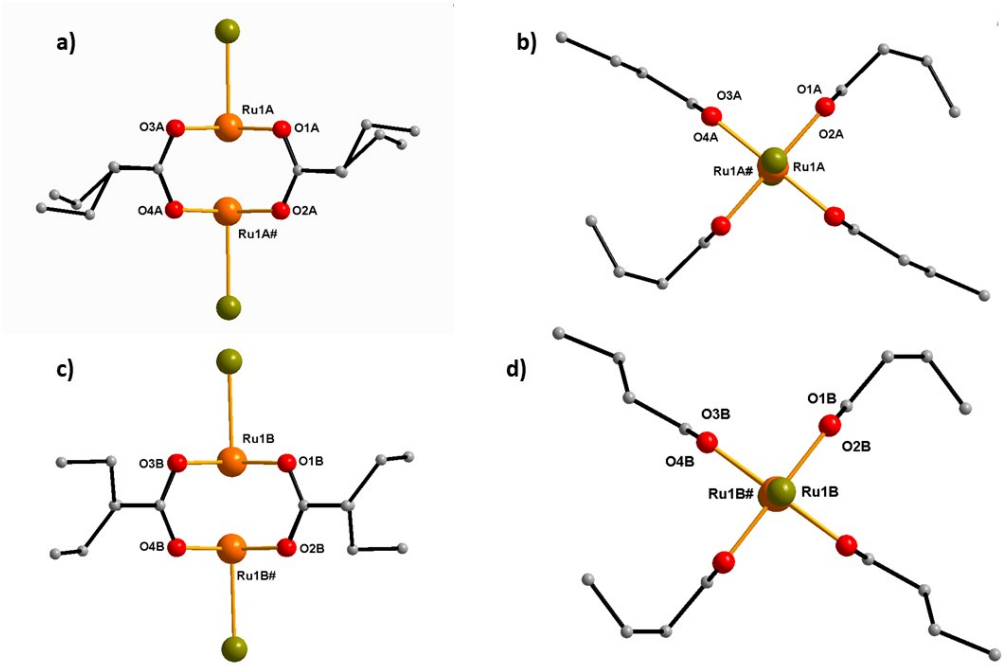

Figure S2: Comparative views of dinuclear complexes A and B showing : a and c) the different conformation of the terminal n-butyl chain of the *n*-butyrato ligands afford by the *cis* and *trans* conformation in A (b) but only *trans*-conformation in B (d).

4. Electron density refinement

In order to model the total electron density, the structure was refined with the independent atom model (IAM) approximation, following by multipolar refinement with the program MoPro [7] using the Hansen and Coppens formalism[8]. The least-squares multipole refinement was performed on 26962 reflections with $I > 5\sigma(I)$. In this work, the atomic position and thermal displacement parameters of non-hydrogen atoms were first refined for high angle reflections (0.8 Å^{-1} < $\sin\theta/\lambda$ < 1.04 Å^{-1}) in order to deconvolute the charge density from structural parameters. Hydrogen atoms were refined at low angles (0.04 Å^{-1} < $\sin\theta/\lambda$ < 0.8 Å^{-1}) and R-H bonds length were restrained to distances tabulated by *Allen et al*.[9]. The multipole parameters were then introduced. Spherical harmonics were used up to octupole (8P) for oxygen atoms, up to hexadecapole (16P) for carbon and nitrogen atoms and up to 64P for bromine and ruthenium atoms. Only monopole and a dipole along the bond were refined at low angles (0.04 Å^{-1} < $\sin\theta/\lambda$ < 0.8 Å^{-1}) for hydrogen atoms. Anharmonicty of 4th and 5th order were tested and refined for Ru et Br atoms on both dimers (A and B) at high order. Single-ξ Slater-type functions used for Ru, Br, C, N, and H were taken from Clementi and Raimondi[10]. The four carboxyl groups were constrained to have identical multipole parameters. The κ and κ′ expansion/contraction set of parameters was constrained to be identical for each unique atom type, depending on their environment, which are assumed to be equivalent. The κ and κ′ constraints of Ru and Br atoms have been released at the end of the refinement and were refined independently. The position of the H atoms and their displacement parameters were refined during the final refinement cycles with all data ($I > 5\sigma(I)$) to check the stability of their restrained positions. The final model with 7049 refined parameters and 26 962 reflections ($I > 5\sigma(I)$) led to R(F)= 0.0287, *w*R(F)= 0.0624 and a goodness-of-fit (g.o.f) equals to 1.058.

Table S3: Final κ and κ’ values (experiment)

	κ	κ’
RuA	1.007(4)	1.20(4)
RuB	1.014(4)	1.42 (5)
BrA	0.956(4)	1.61(5)
BrB	0.9808(4)	1.23 (4)
O1A	0.989(2)	1.03 (5)
O2A	0.998(2)	1.20 (4)
C1A	1.025(5)	0.87 (1)
C2A	0.973(4)	0.90 (2)
C3A	0.918(4)	0.95 (2)
C4A	0.963(3)	0.83 (2)
H	1.106	1.13 (1)

Table S4: Atomic charge of non-hydrogen atoms of dimer A and B

Atom	Charge (e)	Atom	Charge (e)
Ru1A	1.62	Ru1B	1.60
Br1A	-0.14	Br1B	-0.16
O1A	-0.87	O1B	-0.87
O2A	-0.69	O2B	-0.66
O3A	-0.75	O3B	-0.86
O4A	-0.60	O4B	-0.67
C1A	0.37	C1B	0.40
C2A	0.02	C2B	0.53
C3A	-0.33	C3B	-0.14
C4A	-0.08	C4B	-0.72
C5A	0.51	C5B	0.36
C6A	-0.19	C6B	0.06
C7A	0.38	C7B	-0.34
C8A	-0.31	C8B	-0.47

Table S5: Topological parameters at the bond critical points for selected atoms of diruthenium A and B*.

Bond		***dcp*** **(Å)**	***d1cp*** ***(Å)***	***d2cp*** ***(Å)***	**ρ (e.Å $^{-3}$)**	**∇2ρ (e.Å $^{-5}$)**	**λ1 (e.Å $^{-5}$)**	**λ2 (e.Å $^{-5}$)**	**λ3 (e.Å $^{-5}$)**	**ε_{CP}**
Ru1A	Ru1A	2.3107	1.1554	1.1554	0.492	7.735	-1.64	-1.56	10.93	0.05
Ru1B	Ru1B	2.3054	1.1527	1.1527	0.519	8.940	-2.02	-2.01	12.97	0.01
Ru1A	Br1A	2.6557	1.2785	1.3771	0.318	3.253	-0.90	-0.88	5.03	0.02
Ru1A	O1A	2.0287	1.0713	0.9575	0.693	11.342	-3.43	-3.05	17.83	0.12
Ru1A	O3A	2.0253	1.0735	0.9518	0.702	11.252	-3.65	-3.29	18.18	0.11
Ru1B	Br1B	2.6595	1.2788	1.3815	0.315	3.495	-1.02	-1.01	5.56	0.01
Ru1B	O1B	2.0238	1.0795	0.9445	0.720	12.097	-3.82	-3.65	19.57	0.05
Ru1B	O3B	2.0301	1.0831	0.9471	0.711	11.954	-3.74	-3.61	19.31	0.04
O1A	C1A	1.2697	0.8197	0.4502	2.517	-27.285	-24.47	-21.37	18.55	0.14
O2A	C1A	1.2685	0.8177	0.4511	2.514	-27.353	-24.50	-21.43	18.58	0.14
O3A	C5A	1.2694	0.8185	0.4512	2.458	-25.523	-22.79	-21.88	19.15	0.04
O4A	C5A	1.2697	0.8107	0.4592	2.439	-25.809	-22.12	-21.16	17.46	0.05
O1B	C1B	1.2718	0.8103	0.4615	2.492	-26.122	-22.26	-20.54	16.67	0.08
O2B	C1B	1.2744	0.8117	0.4628	2.434	-24.240	-21.58	-19.94	17.28	0.08
O3B	C5B	1.2675	0.8199	0.4477	2.522	-26.818	-24.42	-21.71	19.31	0.13
O4B	C5B	1.2710	0.8158	0.4554	2.496	-28.033	-24.15	-21.23	17.34	0.14
C1A	C2A	1.5054	0.7682	0.7373	1.748	-13.843	-12.35	-11.38	9.89	0.09
C1B	C2B	1.5053	0.7738	0.7316	1.815	-18.366	-14.24	-12.89	8.76	0.10
C2A	C3A	1.5265	0.7535	0.7730	1.744	-13.791	-11.45	-10.91	8.57	0.05
C2B	C3B	1.5255	0.7564	0.7691	1.752	-16.102	-12.33	-11.70	7.93	0.05
C3A	C4A	1.5192	0.7766	0.7427	1.736	-13.020	-11.08	-10.48	8.54	0.06
C3B	C4B	1.5256	0.7710	0.7546	1.826	-18.339	-13.07	-12.49	7.23	0.05
C5A	C6A	1.5109	0.7711	0.7400	1.561	-8.979	-11.21	-7.86	10.09	0.4270
C5B	C6B	1.5083	0.7709	0.7376	1.736	-13.490	-12.34	-11.12	9.96	0.1095
C6A	C7A	1.5169	0.7871	0.7340	1.407	-3.988	-9.41	-3.50	8.92	1.6893
C6B	C7B	1.5215	0.7532	0.7684	1.742	-13.922	-11.85	-10.54	8.47	0.1239
C7A	C8A	1.5279	0.7182	0.8203	1.409	-6.366	-7.48	-6.75	7.86	0.1076

*dcp is the length of the pathway between atom 1 and 2, d1cp is the distance between atom 1 and the bond critical point position and d2cp is the same between atom 1 and the bond critical point position.

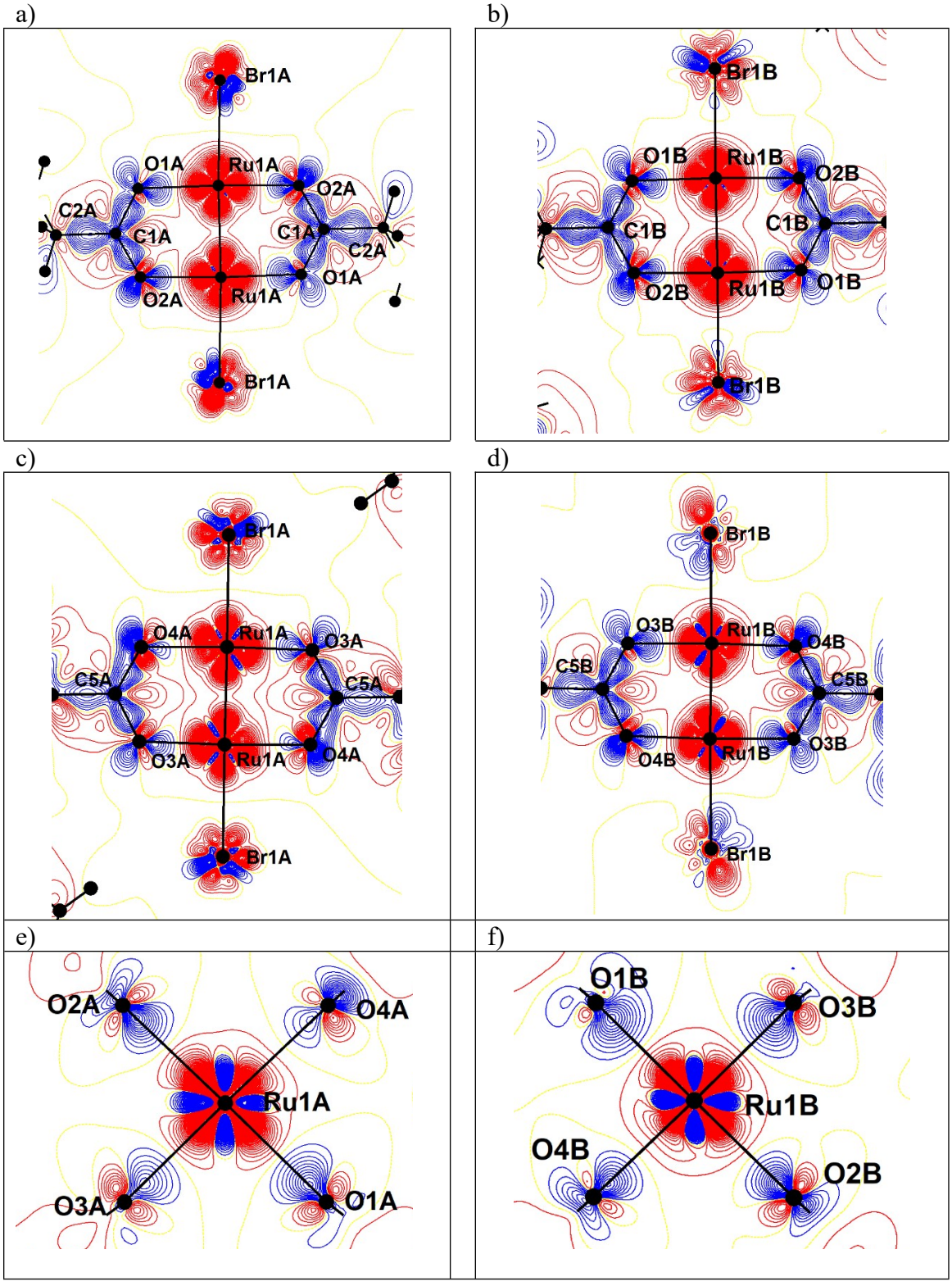

Figure S3: Static deformation density map in different planes. (a) Ru1A-O1A-O2A, (b) Ru1B-O1B-O2B, (c) Ru1A-O1A-Br1A plane, (d) Ru1B-O1B-Br1B, (e) Ru1A-O3A-Br1A, (f) Ru1B-O3B- Br1B. The contour interval level is 0.05 e. $Å^{-3}$. Red lines: negative; Blue lines: positive

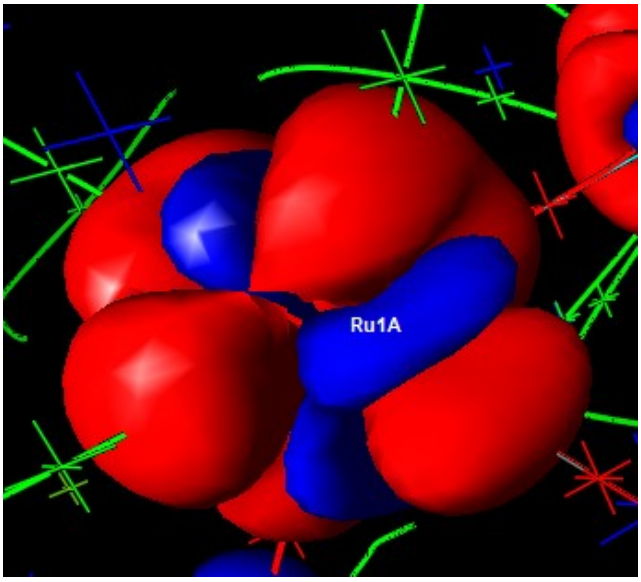

Figure S4: 3D static deformation density map of Ruthenium 1A, isocontours of 0.2 e. $Å^{-3}$; red: negative; blue: positive.

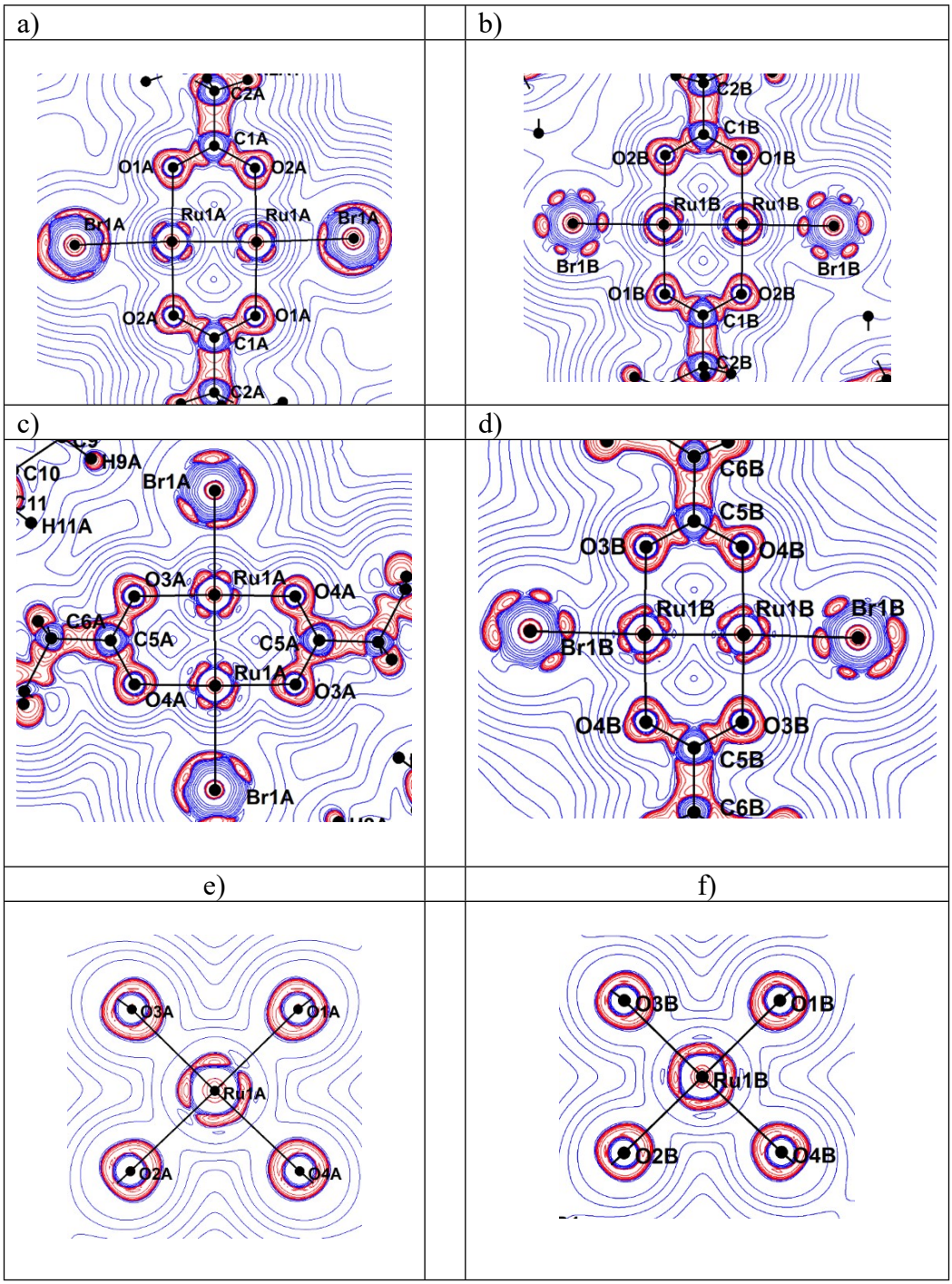

Figure S5: Laplacian distribution around Ruthenium atoms in different planes. a) Ru1A-O1A-O2A; b) Ru1B-O1B-O2B; c) Ru1A-O1A-Br1A plane; d) Ru1B-O1B-Br1B; e) Ru1A-O3A-Br1A; f) Ru1B-O3B- Br1B. The contour levels are at ± 2, 4, 8×10n with n = -1, 0, 1, 2. Red lines: negative; Blue lines: positive

5. Magnetic measurements

Magnetic measurements were performed with a Quantum Design SQUID magnetometer. Magnetic measurements on a polycrystalline sample were done using a polycarbonate capsule as container blocked in straws. Angle-resolved susceptibility measurements were done at 2 K using a rotator for angular resolved measurements on the faces-indexed single crystal used for neutron studies (3.5*2.5*1.5 mm^3) under a magnetic field of 0.1T. The orientation of the crystal on the magnetometer was set manually: **Set 1**: the crystal was set with **a** axis along the rotation axis; **Set 2**: the crystal was set with the ***b*** axis along the rotation axis. In both cases, the ***b*** axis was initially roughly set perpendicular to the magnetic field (rotation angle $\Phi = 0$). Experimental data were simulated from PND results with program CalcM.[11]

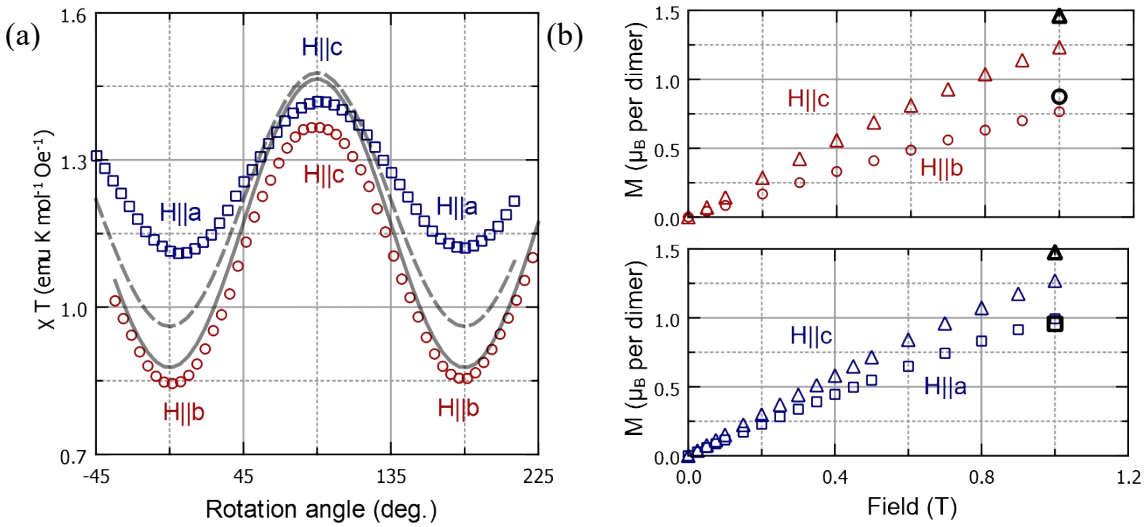

Figure S6: (a) Dependence of the product of the magnetic susceptibility with temperature (χT) with the rotation angle around the axis ***a*** (red circles) and the axis ***b*** (blue squares) at 2K under 0.1T. Straight and dashed lines are simulation based on the PND results. (b) Field dependence of the magnetization at the rotation angle corresponding to maximum and minimum χT value around the axis ***a*** (red symbols) and the axis ***b*** (blue symbols). These parameters estimated from PND measurements at 2K and 1T are given by black lines (a) and black symbols (b).

6. Spin density refinement and magnetic susceptibility tensors determination

6.1. Non-polarized neutron diffraction.

The precise low temperature structure of **1** has been determined, collecting integrated nuclear intensities at 2K on the 4-circle non-polarized neutron diffractometer D19 at the Institut Laue-Langevin (ILL), with a wavelength of 0.950 Å and a large single-crystal (3.5x2.5x1.5 mm^3). The details of the data collection are reported in Table S1. The low temperature structure was refined on 15283 reflections starting from the structure obtained by X-ray diffraction at 100K and with the SHELXL program 2018 version using the $OLEX_2$ software [5-6]. The scale factor and extinction parameter were refined together with the position parameters and isotropic thermal factors for all atoms using no restraints. Main crystal data and structure refinement parameters for neutron diffraction experiment at 2K are displayed in Table S1 and corresponding selected interatomic distances and angles are listed in Table S6. CCDC deposition number 2519322 contains the supplementary neutron crystallographic data for this paper. These data can be obtained free of charge via www.ccdc.cam.ac.uk/data_request/cif, or by emailing data_request@ccdc.cam.ac.uk, or by contacting The Cambridge Crystallographic Data Centre,12 Union Road, Cambridge CB2 1EZ, UK; fax: +44 1223 336 033.

Table S6. Selected interatomic distances (Å) and angles (°) at 2K from neutron diffraction.

Ru1A	Ru1A$^{\#}$	2.3232(18)	Ru1B	Ru1B$^{\#}$	2.3088(17)
Ru1A	Br1A	2.6567(14)	Ru1B	Br1B	2.6599(13)
Ru1A	O1A	2.0353(14)	Ru1B	O1B	2.0265(14)
Ru1A	O2A^{1}	2.0424(14)	Ru1B	O2B^{2}	2.0368(14)
Ru1A	O3A	2.0262(14)	Ru1B	O3B	2.0410(15)
Ru1A	O4A^{1}	2.0404(14)	Ru1B	O4B^{2}	2.0375(15)
O1A	C1A	1.2717(15)	O1B	C1B	1.2688(15)
O2A	C1A	1.2742(15)	O2B	C1B	1.2755(14)
O3A	C5A	1.2762(16)	O3B	C5B	1.2692(15)
O4A	C5A	1.2700(15)	O4B	C5B	1.2752(14)

O1A	Ru1A	Br1A	93.07(5)	O1B	Ru1B	Br1B	91.25(5)
O1A	Ru1A	O2A^{1}	177.68(7)	O1B	Ru1B	O2B^{2}	177.90(6)
O1A	Ru1A	O4A^{1}	87.69(6)	O1B	Ru1B	O3B	90.51(6)
O2A^{1}	Ru1A	Br1A	89.11(5)	O1B	Ru1B	O4B^{2}	88.53(6)
O3A	Ru1A	Br1A	91.61(5)	O2B^{2}	Ru1B	Br1B	90.74(5)
O3A	Ru1A	O1A	91.39(6)	O2B^{2}	Ru1B	O3B	88.85(6)
O3A	Ru1A	O2A^{1}	87.73(6)	O2B^{2}	Ru1B	O4B^{2}	92.04(6)
O3A	Ru1A	O4A^{1}	177.72(6)	O3B	Ru1B	Br1B	89.53(5)
O4A^{1}	Ru1A	O2A^{1}	93.11(6)	O4B^{2}	Ru1B	O3B	177.88(6)
O4A^{1}	Ru1A	Br1A	90.52(5)	O4B^{2}	Ru1B	Br1B	92.38(5)
Ru1A1	Ru1A	Br1A	177.24(6)	Ru1B^{2}	Ru1B	Br1B	178.15(6)

^{1}-x,1-y,2-y; ^{2}1-y,-Y,1-z

6.2. Polarized neutron diffraction.

PND measurements were performed on the same large single-crystal used for non-polarized neutron diffraction and angle-resolved magnetic measurements on the D3 diffractometer at the ILL. Flipping ratios were collected at 2K. The neutron wavelength was fixed at λ= 0.832Å (Heusler alloy monochromator) with a polarization of the incident neutron beam P= 0.95.

To determine the magnetic susceptibility tensors, a magnetic field of 1T was successively applied to the sample along three different directions with respect to the crystallographic axes, respectively along ca. the ***a*** axis, ***c**** axis and ***c*** axis. Measurements were also done at 9T for two of these orientations.

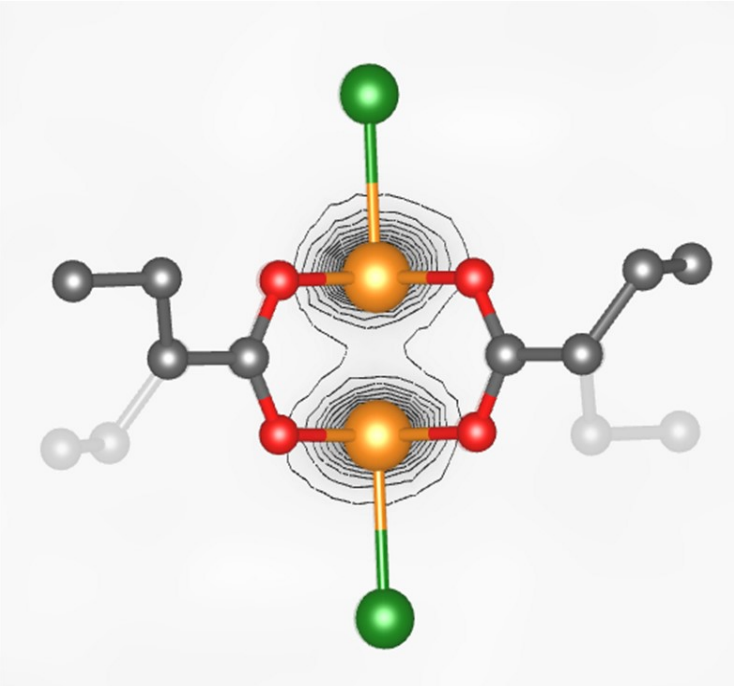

Figure S7: Experimental spin density in at 2 K in a field of 9 T for dimer B with projection around the Ru-Ru bond. Contour levels are fixed at 0.035μ_B/A^3. ??? pas certain au vu du commentaire de Iurii

7. Quantum mechanical calculations

7.1. Methods

All the calculations have been performed using the experimental crystallographic data from single-crystal X-ray diffraction experiment (CCDC: 2516707). Though formally this structure belongs to the C_1 symmetry point group, the $[Ru_2Br_2O_8]^-$ core is close to a D_{4h} symmetric structure. All the results reported in the main text arise from the A diruthenium complex. Results for site B diruthenium complex are reported below Due to the little structural changes occurring between both structures, no much change in the computed properties are found in the B diruthenium complex as may be expected. The ORCA code, version 5.0.4, has been used for all the calculations.[12]

For accounting for both non-dynamic and dynamic correlation effects, complete active space self-consistent field (CASSCF)[13] and post-CASSCF calculations have been performed. We have used the all-electron SARC-DKH-TZVP basis set [14]for the Ru atoms and recontracted Karslruhe basis sets for the lighter atoms[14]: DKH-def2-TZVP for Cl, DKH-def2-SVP for C and DKH-def2-SV for H. The Douglas-Kroll-Hess Hamiltonian [15] (at second order) is used to account for the scalar relativistic effects. The active space consists in 11 electrons within 10 orbitals, *i.e.* in the d electrons and orbitals. To compute the spin-orbit free *effective* bond order [16],a state-specific calculation concerning the ground $S = 3/2$ state has been performed.

In view of computing the zero-field splitting parameters, the *contracted* spin-orbit configuration (SOCI) method has been used. It consists in diagonalizing the electronic energy plus spin-orbit coupling matrix in the basis of the spin components of a set of spin-orbit free states. Two main degrees of freedom appear: the definition of the set of states (full CAS *vs.* subset of it) and the correlation level that is used to obtain the electronic energies. Since we use a state-average scheme to compute the initial set of spin-orbit free states, enlargement of this set adds extra spin-orbit coupling interactions on the one side and more averaging artifacts on the other side [17]. By experience, the CASSCF energies may not be precise enough to “dress” the diagonal

elements of the SOCI matrix and it is common practice to use more correlated energies obtained at least at a multireference second-order perturbation theory level. In this work, the strongly-contracted *N*-electron valence states perturbation theory at second-order (NEVPT2) [18] has been used. The spin-orbit coupling matrix elements have been computed in a mean-field fashion [19].

It is important to check the convergence of the zero-field splitting parameters with respect to the size of the SOCI matrix. We have used three spaces of increasing size, consisting in the spin components of 9 $S = 1/2$ and 4 $S = 3/2$ states (smaller space), 16 $S = 1/2$ and 13 $S = 3/2$ states (intermediate space) and 17 $S = 1/2$ and 15 $S = 3/2$ and 2 $S = 5/2$ states (larger space). The resulting axial zero-field splitting D parameters are 94, 94 and 104 cm^{-1}, respectively. The perfect agreement in the first two space in fact hides significant changes in the state-by-state contributions and thus our intermediate space is in fact the best compromise of the three since it correctly includes the most contributing states while limiting the magnitude of the averaging artifacts. This is why it is the space that was retained for the production calculations that are reported in the main text.

Finally, the fact that the rhombic E parameter is quite small (2 cm^{-1}) is in perfect line with the close to D_{4h} symmetry of the magnetic core (the paramagnetic centers plus the atoms belonging to their first coordination spheres).

7.2. Results for B diruthenium complex

- Electronic structure of the ground state: $\pi^{3.76}\sigma^{1.88}\delta^{1.86}\delta^{*1.14}\pi^{*2.22}\sigma^{*0.12}\delta^{0.01}\delta^{*0.01}$

- Effective bond order: 2.01.

- Lowest spin-orbit free excitation energies: 0.92 eV for the first excited $S = 3/2$ state and 0.30 eV for the first $S = 1/2$ state.

- Splitting between the first Kramers doublets KD1 and KD2: 186 cm^{-1} (23.0 meV).

- Summed weights for the spin components of the ground $S = 3/2$ state: 96.8 % for KD1 and 98.9 % for KD2.

- Zero-field splitting parameters: $D = 93$ cm^{-1} and $E = 1$ cm^{-1}.

References

[1] M. Handa, H. Yairi, Y. Koyama, R. Mitsuhashi, M. Mikuriya, *X-ray Struct. Anal. Online* **2022**, *38*, 21-23.

[2] Agilent, Agilent Technologies Ltd, Yarnton, Oxfordshire, England, **2014**.

[3] R. H. Blessing, *Crystallogr. Rev.* **1987**, *1*, 3-58.

[4] G. M. Sheldrick, *Acta Cryst. A* **2015**, *71*, 3-8.

[5] G. M. Sheldrick, *Acta Cryst. C* **2015**, *71*, 3-8.

[6] (a) L. J. Bourhis, O. V. Dolomanov, R. J. Gildea, J. A. K. Howard, H. Puschmann, *Acta Cryst. A* **2015**, *A71*, 59-71; (b) O. V. Dolomanov, L. J. Bourhis, R. J. Gildea, J. A. K. Howard, H. Puschmann, *J. Appl. Crystallogr.* **2009**, *42*, 339-341.

[7] B. Guillot, L. Viry, R. Guillot, C. Lecomte, C. Jelsch, *J. Appl. Crystallogr.* **2001**, *34*, 214-223.

[8] N. K. Hansen, P. Coppens, *Acta Cryst. A* **1978**, *34*, 909-921.

[9] (a) F. H. Allen, *Acta Cryst. B* **1986**, *42*, 515-522; (b) F. H. Allen, I. J. Bruno, *Acta Cryst. B* **2010**, *66*, 380-386.

[10] E. Clementi, D. L. Raimondi, *J. Chem. Phys.* **1963**, *38*, 2686-&.

[11] O. Iasco, Y. Chumakov, F. Guegan, B. Gillon, M. Lenertz, A. Bataille, J. F. Jacquot, D. Luneau, *Magnetochemistry* **2017**, *3*.

[12] F. Neese, *Wiley Interdisciplinary Reviews-Computational Molecular Science* **2022**, *12*.

[13] B. O. Roos, P. R. Taylor, P. E. M. Siegbahn, *Chem. Phys.* **1980**, *48*, 157-173.

[14] D. A. Pantazis, X. Y. Chen, C. R. Landis, F. Neese, *J. Chem. Theory Comput.* **2008**, *4*, 908-919.

[15] (a) M. Douglas, N. M. Kroll, *Annals of Physics* **1974**, *82*, 89-155; (b) B. A. Hess, *Phys. Rev. A* **1986**, *33*, 3742-3748; (c) G. Jansen, B. A. Hess, *Phys. Rev. A* **1989**, *39*, 6016-6017.

[16] B. O. Roos, A. C. Borin, L. Gagliardi, *Angew. Chem. Int. Ed.* **2007**, *46*, 1469-1472.

[17] R. Maurice, R. Bastardis, C. de Graaf, N. Suaud, T. Mallah, N. Guihéry, *J. Chem. Theory Comput.* **2009**, *5*, 2977-2984.

[18] (a) C. Angeli, R. Cimiraglia, S. Evangelisti, T. Leininger, J. P. Malrieu, *J. Chem. Phys.* **2001**, *114*, 10252-10264; (b) C. Angeli, R. Cimiraglia, J. P. Malrieu, *Chem. Phys. Lett.* **2001**, *350*, 297-305.

[19] F. Neese, *J. Chem. Phys.* **2005**, *122*.